Glass foams for environmental applications

Ronan Lebullenger, Sébastien Chenu, Jean Rocherullé, Odile Merdrignac-Conanec, François Cheviré, Franck Tessier, A. Bouzaza, S. Brosillon

Glass foams for environmental applications

R. Lebullenger[a,*], S. Chenu[a,] J. Rocherullé[a], O. Merdrignac-Conanec[a], F. Cheviré[a], F. Tessier[a], A. Bouzaza[b], S. Brosillon[c]

[a]UMR6226 SCR, Verres et Céramiques, Nitrures, Université de Rennes 1, 35042 Rennes, France
[b]UMR6226 SCR, Chimie et Ingénierie des Procédés, Ecole de Chimie de Rennes, 35708 Rennes, France
[c]UMR Cirad 016, LGPEB, Université de Montpellier 2, 34095 Montpellier Cedex 5, France

** E-mail address: ronan.lebullenger@univ-rennes1.fr*

ABSTRACT : Glass foams were produced using glass industrial waste and aluminium nitride as foaming agent. Steel-making dusts were also used to prepare these expanded materials. Time and temperature process parameters were tuned to adjust physico-chemical properties such as density and porosity. Structural characterisation by X-ray diffraction reveals the amorphous or crystalline nature depending on process parameters. Apparent density varies from 0.2 to 1.2 g cm^{-3} and pycnometric density from 1 to 2.2 g cm^{-3}. The pore nature (close or open) is correlated to the preparation process and the initial batch composition. When doped or coated by titanium dioxide, expanded glasses present a photocatalytic activity in the UV region and were tested for toluene decomposition in gas phase. We have shown that TiO_2-coated foam glasses are efficient, as a support for total toluene photodegradation, in comparison with cellulose/TiO_2 based commercial support.

1. Introduction

Glass recycling is nowadays well implanted in worldwide quotidian lives. In each country, recuperation of glass alimentary containers, windows or cathode ray tube for example is encouraged by European laws. The case of glass waste from automotive industry is not so visible. In general, foam glass prepared from glass cullet needs a milling step to produce a glass powder. The conclusions of studies carried out on the influence of powder granulometry distribution on expanded resulting materials differ from one author to another. The foaming agent is

commonly the calcium carbonate or chalk. Other expansion precursors such as sodium sulphate, mixture of iron oxide with carbon, and also silicium carbide were largely studied [1–11]. However, the use of nitride compound (Si_3N_4 or AlN) which provide the formation of nitrogen bubbles is more “ecologically correct” [12,13]. Expanded glass based materials are commercially available (Corning Pittsburg) for phonic or thermal insulation [14–19]. The photo catalytic support approach could be an added value and a new use of these foam glasses in the civil and building engineering.

The semiconductor photocatalytic activity is based on the adsorption of an ultra band gap photon that promotes an electron from the valence band to the conduction band. In the case of titanium dioxide semiconductor, photon energy must be higher than 3.2 eV for anatase crystalline form that means a photon wavelength below 385 nanometers. The resulting electron–hole pair, after migration at the semiconductor surface, is then available for chemical redox reactions [20]. Particularly, the titanium dioxide modified materials have gained an increasing attention, due to the wide range of possible applications. Moreover, the relative low cost of the photocatalytic active TiO_2 opened the way to scale applications, for example in the building sector. Studies have been reported in literature on various applications, including cementitious materials [20–23].

In recent years, photocatalysis has proved to be a good technique for eliminating many water pollutants [24–27] or air, such as volatile organic compounds (VOCs) [22]. These compounds may be emitted by human activities (transport, industry) but are also present in many products and materials within our homes. VOCs include a variety of substances that may be of biogenic origin (natural) or anthropogenic (human origin). They contain always the carbon element and other elements such as hydrogen, halogen, oxygen, and sulphur.

The aim of this present work is to prepare and characterise glass foams obtained from ordinary glass waste from automotive industry with the objective to be used as photocatalytic support. A preliminary comparison of the photocatalytic activity between TiO_2 coated foam glasses and commercial impregnated cellulose support is also presented, studying the decomposition of gaseous toluene under UVA illumination.

2. Experimental procedure

2.1. Foam glass preparation

Previous research developed in our laboratory was realised on glass powdered and aluminium nitride [2–4,12,13]. In this present study, we used industrial glass waste formed by glass micro spheres of 250 μm diameter. These glass micro balls are contaminated by oil and rubber impurities from the manufacturing process where they were used as heat transfer media for the rubber vulcanisation step in the automotive industry. The chemical glass sphere composition is in

weight percent: 72.5 SiO_2–13.7 Na_2O–9.8 CaO–3.3 MgO–0.4 Al_2O_3–0.2 FeO/Fe_2O_3–0.1 K_2O. The foaming agent used in the experiments is aluminium nitride from H.C. Starck GmbH. Glass micro balls are mixed with aluminium nitride, and the resulted initial batch of 1 kg weight is introduced in a refractory nickel steel mould. Some foam samples were prepared by adding to the initial batch, titanium dioxide P25 from Degussa or dust residues from blast furnaces provided by Arcelor Mittal Dunkerque (France). The thermal treatment of the mixtures is performed in a conventional electrical furnace. The heating rate is about 15 K min^{-1} and the dwell temperature is maintained for one to four hours. The cooling rate of the obtained foam material is governed by the furnace inertia.

2.2. Foam glass characterisation techniques

Differential thermal and gravimetric analyses (DTA–TGA) were carried out on TA Instruments Model SDT 2960 equipment. Measurements were done under synthetic air, using platinum crucibles and a 10 K min^{-1} heating rate. X-ray diffraction characterisation conducted on crushed samples was realised at room temperature with a Philips PW3710 diffractometer operating with Cu Kα radiation (λ = 1.5418 Å), the counting step and time were 0.02 ° and 1 second respectively. X'PERT softwares – Data Collector and Graphics and Identify – were used, respectively, for recording, analysis, and phase matching of the patterns. Helium picnometer AccuPyc 1330 Micromeritics was used to determine the samples density. Nitrogen and oxygen content in foam glasses was determined with a LECO TC-436 analyzer using the inert gas fusion method. Oxygen is measured as CO_2 by infrared spectroscopy, while the nitrogen released as N_2 , is determined by thermal conductivity.

2.3. Catalyst supports

The glass foams previously prepared (sample#8 ones, see Table 1) were used as support for photocatalysis tests. The amount of titanium dioxide required to deposit on glass foam is placed in a water/alcohol mixture (50/50) to form a slurry solution [28]. Three different slurries for deposit were prepared to coat 350 cm^2 of foam plates. That means quantities of 0.7, 1.4 and 2.1 g of TiO_2 PC500 from Millenium were dispersed in a 50 ml volume of a water/alcohol mixture to prepare coated samples with 20, 40 and 60 g of TiO_2/m^2, named Foam20, Foam40 and Foam60 respectively. The slurry is wholly deposited on each foam samples with a brush. We verified that the TiO_2 coating was better controlled with the brush method than the spray application. In our study, the titanium dioxide used is PC500 reference provided by the Millennium Society (pure anatase crystalline phase). The coated foam glass pieces are then heat treated at 560 °C to insure a good TiO_2 adhesion. The commercial media used for comparison is the “media 1049”, composed of cellulose fibres coated with silica and titanium dioxide (PC500). This catalyst support is flexible and provided by Alhstrom Paper Group. The quantity of catalyst deposited on the media is equal to 25.5 g m^{-2}. A 480 cm^2 sheet impregnated commercial paper is placed in the reactor for this study. Specific area of studied powders was measured by BET technique with Micromeritics Flowsorb II 2300 equipment.

2.4. Photocatalysis experimental setup

The reactor used in this study is a batch reactor type of 1.5 l capacity. The commercial media catalyst or the coated foam glass is placed in the reactor. The UV lamp used for catalyst illumination is a compact fluorescent lamp provided by Philips under the reference “PL-L 24 W/10/4P”, its spectrum is centred at λ_{max} = 365 nm for a power average of 27 W/m^2 measured with a radiometer (Vilber Lourmat, VLX-3W). The reactor is sealed, and a small volume (micro litre, µl) of liquid toluene (Carlo Erba Reagenti) is injected through the septum using a syringe. The vaporisation of toluene occurs instantaneously. Before irradiation, the air–toluene mixture is stirred with a magnetic bar during at least 1 h in the dark. We note a decrease of the concentration during the first minutes. This is due to the adsorption, on the catalyst surface, which is the first step of the heterogeneous catalysis. After 50 min, the equilibrium adsorption is reached. The concentration of gaseous toluene in the reactor is followed by sampling and gas chromatography analysis. Then the UV lamp is switched on to initiate the photo degradation. Toluene samples are taken every 3 min using 1000 µL chromatographic syringe. The analysis is done by gas chromatography (Fisons GC 9000 series) equipped with a capillary column (Chrompact FFAP-CB) and a flame ionization detector. Nitrogen is used as a gas-carrier (P = 50 kPa). The temperature conditions for the oven, the injection chamber and the detector are respectively 115, 200 and 250 °C. Under these conditions of analysis, the retention time of toluene is 1.30 min.

3. Results

3.1. Thermal and structural characterisation of glass foams

Fig. 1 shows the curves obtained for the DTA–TGA measurement performed under air on aluminium nitride used as foaming agent. We have observed a first small exothermic peak with onset temperature about 800 °C followed by a second high one with a maximum at 1200 °C. These peaks correspond to AlN oxidation as explained in the discussion

part. Fig. 2 presents the DTA curve obtained on a 50 mg mixture of glass micro balls waste with 2% weight of aluminium nitride. The glass transition is observed at 560 °C and an exothermic peak is present at 850 °C revealing the decomposition reaction of AlN with the viscous glass melt. We have also realised thermal analysis (not showed here) on foam samples and its glassy nature is confirmed by the presence of an endothermic step (glass transition) around 560 °C. For the sample prepared with a dwell of 4 h, a partial devitrification is highlighted by the presence of diffraction peaks on XRD patterns (Fig. 3). The crystallised phases identification with X'PERT software revealed the presence of numerous possible phases including mainly wollastonite ($CaSiO_3$ — ICDD-PDF#27-0088) and SiO_2 (#14-0654 and #11-0695) [29].

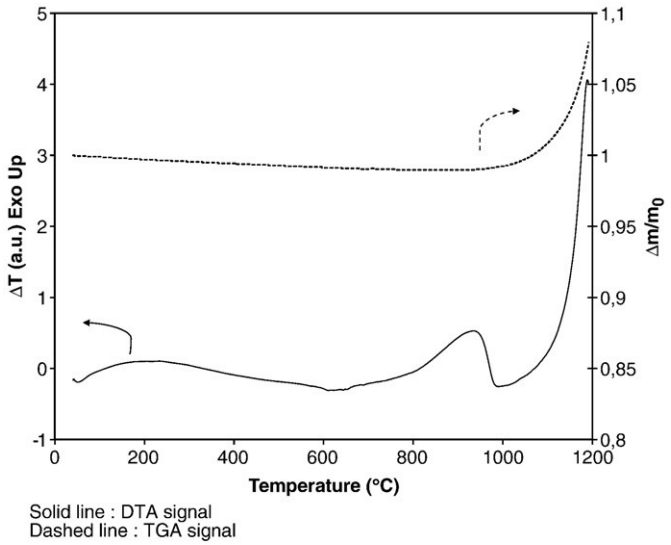

Fig. 1. DTA–TGA curves obtained for AlN under air.

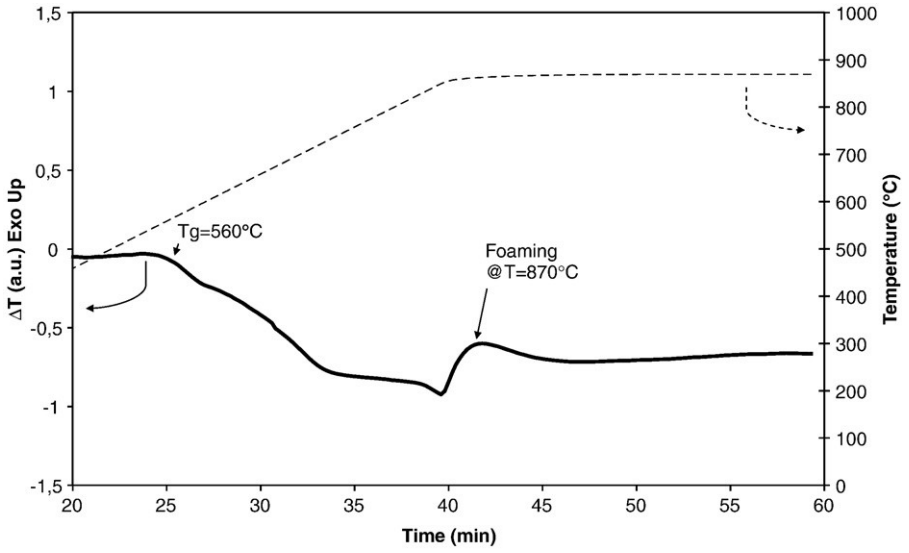

Fig. 2. DTA curve (in function of time) for a glass–AlN mixture (98–2 wt.%).

3.2. Density and chemical composition of glass foams

Table 1. Initial batch composition, process parameters, and characteristics of prepared foam samples.

Sample #	Initial batch					T (°C)	Time (min)	Foam sample				
	Glass (wt.%)	AlN (wt.%)	N (wt.%) calcul.	TiO_2 (wt%)	Steel waste (wt.%)			D_{pyc} (g cm^{-3})	D_{app} (g cm^{-3})	Closed porosity (vol%)	Open porosity (vol%)	$N_{residual}/N_{initial}$ (wt.%)
1	98	2				800	90	1.215	1.18	50	3	
2	98	2				820	90	0.971	0.80	50	18	
3	98	2				820	240	2.293	0.70	3	69	
4	98	2				850	90	1.369	0.49	16	64	
5	98	2	0.68			850	120	2.222	0.63	3	72	80
6	98	2	0.68			850	240	2.310	0.66	2	71	74
7	95.5	1.5	0.51	3		850	120	2.278	0.69	3	70	74
8	95.5	1.5	0.51	3		850	240	2.316	0.42	1	82	66
9	95.5	1.5			3	850	240	2.308	0.47	2	80	
10	95.5	1.5		1.5	1.5	850	240	2.303	0.41	1	82	
11	98	2				880	90	1.704	0.37	7	78	
12	91	3		6		900	240	2.108	0.29	2	86	

d_{pyc} : pycnometric density.
d_{app} : apparent density.

Table 1 summarizes the values of density and porosity as well as the chemical composition (nitrogen analysis) of foam glasses prepared at different temperatures and times. The density values were obtained by helium pycnometry (d_{pyc}) as well as from weight and apparent volume measurements (d_{app}). If we consider that the total volume (V_f) of a foam sample is the sum of glass matter volume (V_g), open pores volume (V_o) and close pores volume (V_c), we propose to express the different densities (in g cm^{-3}) as following. For pycnometric density, we obtain $d_{pyc} = m/(V_g + V_c)$, where m is the weight of the foam sample. For apparent density, we get $d_{app} = m/V_f$ or $d_{app} = m/(V_g + V_c + V_o)$. Open porosity, i.e. V_o/V_f (%) can be described by the following formula: Open porosity $= (1 - d_{app}/d_{pyc}) \times 100$. Closed porosity, i.e. V_c/V_f, (%) can be expressed by: Closed porosity $= (d_{app}/d_{pyc} - d_{app}/2.5) \times 100$, where 2.5 is the estimated medium value of density in g cm^{-3} of the glass without pores (m/V g = 2.5). In Table 1 are reported the calculated values of open and closed porosity.

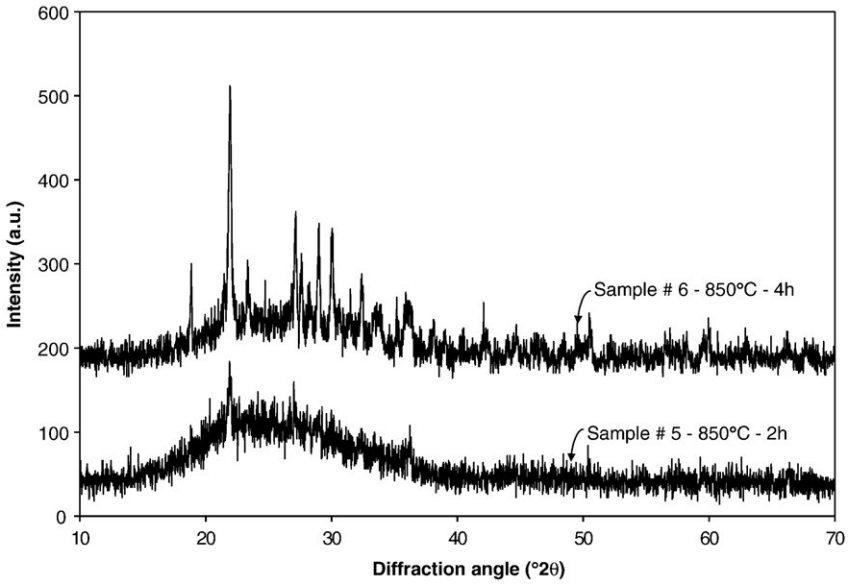

Fig. 3. X-ray diffractograms for samples prepared at 850 °C for 2 and 4 h.

For samples with the same initial composition (sample#1, #2, #4 and #11), the pycnometric values tends to increase with the temperature from 800 to 880 °C whereas the apparent density is decreasing from 1.18 to 0.37 g cm^{-3}. These results lead to an increase of open porosity from 3 to 78%, meaning the connection of nitrogen bubbles in the viscous melt with temperature increase. It can be observed that the increase of heat treatment time has the same effect than the temperature increase (#2 and #3 treated at 820 °C; #4, #5 and #6 treated at 850 °C). The addition of TiO_2 (#8), or steel dust (#9) or both (#10) treated in the same conditions (850 °C for 240 min) also lead to high porosity, 82, 80 and 82% respectively. However, the highest porosity (86%) was obtained for the sample with 6% TiO_2 heated at 900 °C during 240 min (#12). In addition, the highest pycnometric values are close to 2.3 but are lower than of initial glass beads (d_{glass} = 2.48 g cm^{-3}) revealing the presence of closed pores inside the foamed samples.

The oxygen and nitrogen analysis was performed on crushed foam samples. The nitrogen content measured is from the N^{3-} ion nitrides still present in the foam material. As shown in Table 1, only 20 to 30% of the nitrogen introduced with AlN in the initial batch has reacted and participated in the expansion of the glass. An increase in reaction time yields for better use of the pore-forming agent. Similarly, the addition of titanium dioxide promotes the decomposition of aluminium nitride.

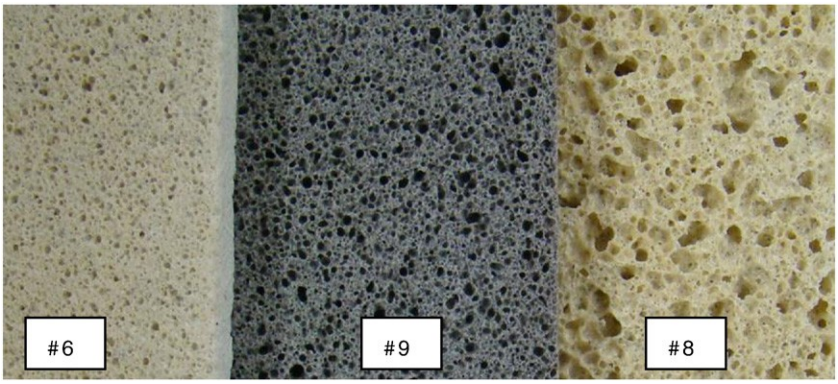

Fig. 4. Photography of foam glasses prepared at 850 °C for 4 h, (#6: glass + AlN; #8: glass + AlN + TiO_2 ; #9: glass + AlN + steel waste).

Fig. 4 shows photography of some foam samples prepared in the same conditions (850 °C for 4 h). Sample #6 presents a white colour while, sample #9 containing iron oxide is grey and a yellowish tint is observed for sample #8 containing TiO_2. It can be also observed that iron and titanium doped foams present bigger pores (few millimetres diameter) for identical experimental parameters such as time and temperature.

3.3. Characterisation of TiO_2 used for the coating of glass foams

The catalyst powder TiO_2 PC500 from Millenium was dispersed in water/ethanol slurry, and then was dried up to 550 °C. This operation was realised with the aim to know the influence of thermal treatment of coated foam on its catalyst properties. X-ray diffraction analysis showed that the anatase structure of PC500 TiO_2 is kept even after the 550 °C treatment. We observed a narrowing of the width at half height for the diffraction peaks. The specific area measured by BET analysis confirmed the thermal effect and we observed a drastic decrease of the specific area value from 260 to 60 $m^2 g^{-1}$. On the other hand, it was not possible to measure the specific area of the commercial media 1049, because this material cannot support a treatment above 250 °C, this drying step being necessary before BET analysis.

The coated foams were observed by scanning electronic microscopy (Fig. 5). The coating presents some cracks, but for catalysis applications it is an advantage because these defects will increase the contact surface with toluene. The nature of the solution used to prepare the slurry had influence of the coating adhesion. Adhesive screen test revealed that the mixture H_2O/ethanol (50/50) was the best compared with pure solution of water or alcohol.

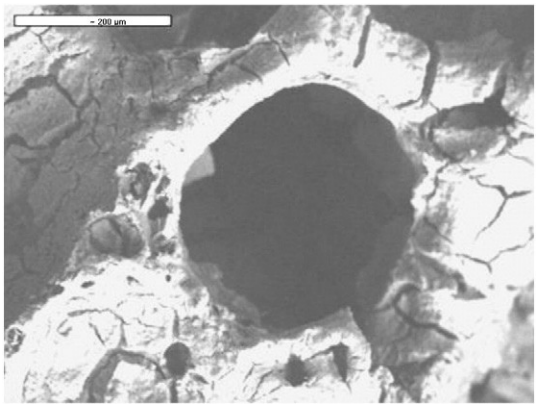

Fig. 5. SEM picture of a TiO_2 coated glass foam.

3.4. Photocatalysis of toluene

To study UVA photocatalytic degradation of toluene, various initial concentrations of toluene were tested with the different catalyst supports. For each toluene degradation runs, we wait systematically 1 h before initiating the UV illumination of the catalyst, and we observed that a portion of introduced toluene was adsorbed by the catalyst. The adsorption capacity at the equilibrium, Q_e (mg g^{-1}), is equal to $(C_0 - C_e)\cdot V/w$, where C_0 is the initial injected toluene concentration (mg m^{-3}), C e is the equilibrium toluene concentration (mg m^{-3}), V is the volume of the batch reactor (1.5 litre) and w is the mass (g) of TiO_2 deposited on the considered support. Fig. 6 presents the evolution of Q_e in function of initial toluene concentration C_e for the three studied supports (Foam20, Foam40 and Media1049). We note that the adsorption capacity increases with the concentration of toluene in the reactor. This behaviour seems to be a Langmuir type. One can note that the adsorption on coated foams is negligible when compared with media 1049.

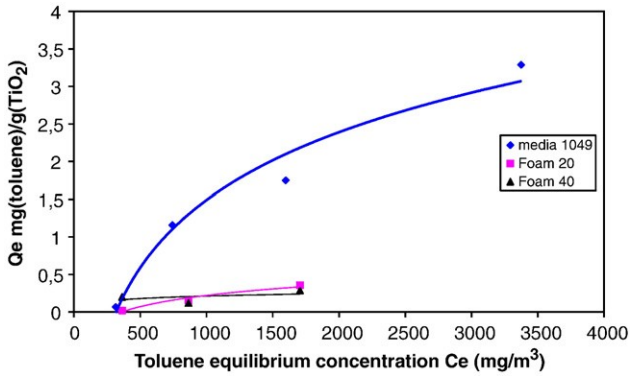

Fig. 6. Adsorption capacity at the equilibrium Q_e (mg g^{-1}) versus equilibrium toluene concentration C_e (mg m^{-3}) for three supports (Foam20, Foam40 and Media 1049).

Fig. 7 shows the evolution of toluene concentration with illumination time for the four studied supports. The initial concentration at time equal to zero is the one measured after the 60 min of the adsorption step. For Foam20 support (20 g of TiO_2 by m^2), an initial toluene concentration of 1500 mg m^{-3} was completely degraded after 30 min (Fig. 7a). Regarding support Foam60 (60 g of TiO_2 by m^2), the degradation time is reduced to 20 min (Fig. 7c). Therefore, the higher the catalyst coating concentration is, the faster is the toluene degradation. This observation is in accordance with an heterogeneous photocatalysis mechanism. For commercial media 1049 (25.5 g of TiO_2 by m^2), 25 min are necessary to decompose the same toluene initial concentration (1500 mg m^{-3}) (Fig. 7d). However, the different supports did not contain the same amount of catalyst depending on the TiO_2 concentration and size of the support. For better comparison, we calculate the apparent rate of degradation, taking into account the total amount of titanium dioxide for each support. Using the Langmuir–Hinshelwood model, described in details elsewhere [25–27], and applying it to the results obtained for different initial concentration of toluene (mg m^{-3}) and different TiO_2 catalyst concentration (g m^{-2}), we determined the apparent rate of toluene degradation, k_2, expressed in mg m^{-3} min^{-1} g^{-1}. For commercial support, the quantity of titanium dioxide was 1.2 g (480 cm^2 × 25.5 g m^{-2}). For coated foams, we used a surface of 350 cm^2 with 20, 40 or 60 g m^{-2} TiO_2 concentration. The k_2 values obtained are listed in Table 2. Thus, it may be observed that support foam (60 g m^{-2}) presents an apparent constant rate of degradation of toluene comparable to TiO_2 Media 1049, namely 400

(mg m^{-3} min^{-1} g^{-1}). However, it is possible that all the TiO_2 deposited on the foam is not used for photocatalysis. Therefore, additional tests are needed to confirm the efficiency of these coated supports.

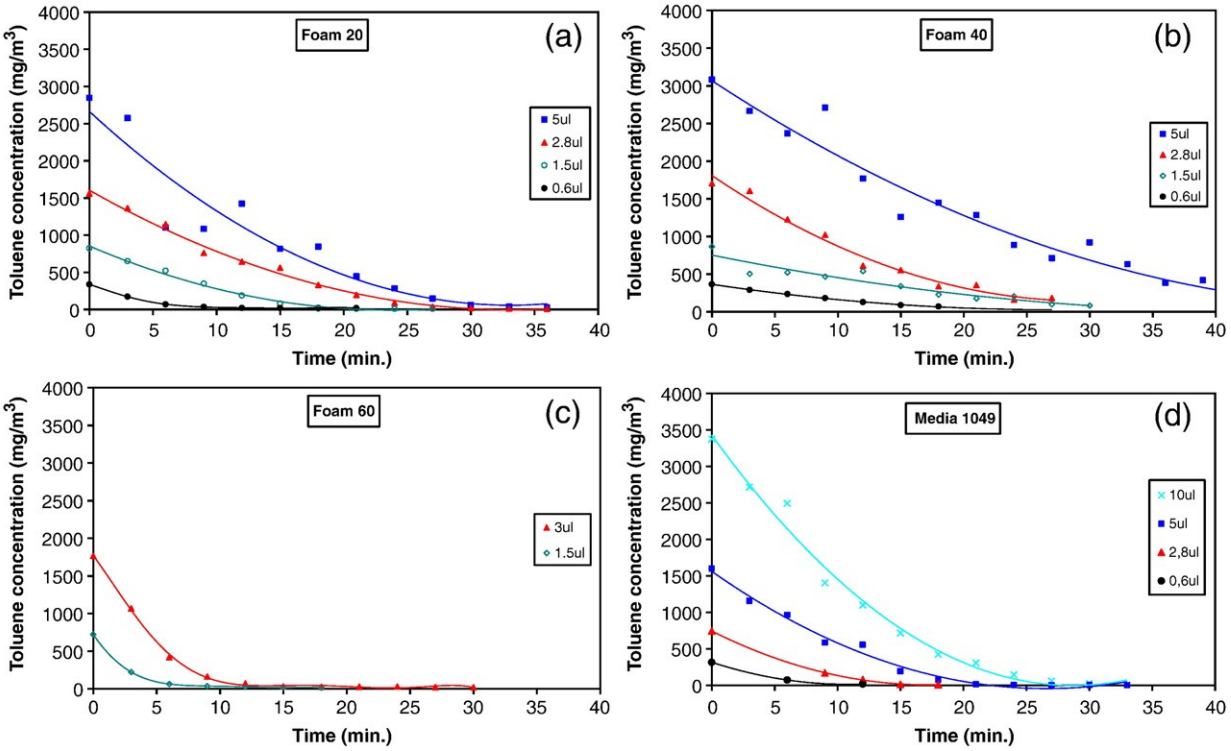

Fig. 7. Evolution of toluene concentration in function of UVA illumination time for the four studied support (Foam20, Foam40, Foam60 and Media1049). The initial volume (microlitre, µl) of toluene injected in the batch reactor is indicated in the graph inserts.

Table 2. Apparent rate of toluene degradation for coated supports with 20, 40, 60 g of TiO_2/m^2 and Media1049 (25.5 g m^{-2}).

	Foam 20	Foam 40	Foam 60	Média 1049
k_2 (mg(toluene)/m^3/min/g(TiO_2))	172	278	400	385

4. Discussion

The foaming process results of the AlN decomposition reaction occurring between 800 and 1200 °C (Fig. 1) and can be written as following:

$$2AlN(s) \rightarrow 2Al(s) + N_2(g). \quad (1)$$

The reduced aluminium Al is oxidized by the oxygen present in the glass, and the alumina produced is dissolved in the viscous glass melt. Previous works described that the aluminium nitride oxidation occurs when alkali elements (Na, K) or transition metals (Fe, Mn, Ti) are present as oxide compounds in the melt [13]. Fig. 8 shows the Ellingham diagram for various redox couples.

More generally, the foaming reaction can be described as:

$$3\ M^{n+} + nN^{3-} \rightarrow 3\ M\ +\ n/2\ N_2(g). \quad (2)$$

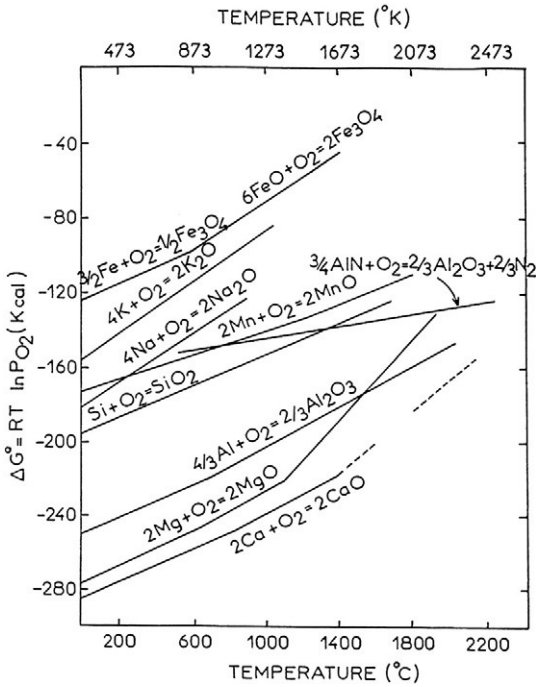

Fig. 8. Ellingham diagram for the oxidation of aluminium nitride and various metals.

Regarding the influence of experimental parameters on the values of porosity, several comments can be made. For foams prepared with AlN at 820 °C, the heating time has an important influence on the closed and open porosity (samples #2 and #3, Table 1). At this temperature, the aluminium nitride oxidation is weakly exothermic as observed in DTA analysis (Fig. 1). For temperatures above 820 °C, the soda–lime silicate glass viscosity is below 10^8 Poises, it corresponds to the working or blowing glass region. So, the nitrogen bubbles from aluminium nitride oxidation can expand more easily and connect themselves. Besides, when increasing process temperature, the aluminium nitride oxidation is also improved (see Fig. 1). The samples prepared at 850 °C present a high open porosity (>70%), available for the penetration of the slurry, also the connection of the pores allows the flow of fluids through the prepared foams, important for the future catalytic performance. At this temperature or above, an increase time does not change drastically porosity because the pore connectivity is yet achieved, and for longer time, devitrification is occurring (Fig. 3). Thus, for catalytic tests, we used foam glasses prepared at 850 °C which is also favourable for the energy balance of the process.

For samples prepared with a mixture of aluminium nitride and titanium dioxide, the presence of TiO_2 enhanced the foaming process (samples #5 and #7 (850 °C – 2 h) and samples #6 and #8 (850 °C – 4 h)).

$$3\ TiO_2 + 4\ AlN \rightarrow 2\ Al_2O_3 + 3\ TiN + 1/2\ N_2 \quad (3)$$

The same improvement is observed for sample containing prepared fly ash. It is due to the presence of iron oxide Fe_2O_3 as reported elsewhere [16].

Concerning the TiO_2 coating process of expanded glasses, investigations are in progress to perform a heat treatment at lower temperature and to study its influence on catalyst adhesion and toluene degradation. Indeed, in heterogeneous catalysis, the catalyst surface in contact with the reactants (active surface) plays an important role on the kinetics of degradation. In addition, the irradiated surface must be the more important as possible since the catalytic reaction is activated by the UV irradiations. So, a catalyst will be more efficient than its active surface is large. The influence of coating parameters such as temperature preparation on catalyst TiO_2 structure (anatase or rutile) or specific area must be implemented to improve these new catalyst supports which are glass foams prepared from industrial wastes.

5. Conclusion

We prepared foam glasses using glass micro balls waste from automotive industry and aluminium nitride as foaming agent. The incorporation of blast furnace smoke or titanium dioxide in the initial batch improves the foaming process. Prepared expanded glasses presented open porosity higher than 70%. Temperature and time influences on foam characteristics were checked and explained. Medium temperature such as 850 °C is sufficient to prepare cellular glasses which were then coated by TiO_2 using a water/alcohol slurry. These coated foams were compared to a commercial catalyst media for the toluene degradation under UV illumination. By analyzing these different materials, we

determined that the coated foam glasses are photoactive. The coated foams, that we analyzed, present a similar effectiveness than commercial photocatalyst paper, but for higher catalyst concentration. However, these first results are very encouraging, and it can be underlined that the glass support presents a strong advantage on cellulose media: after a number of efficient uses, heat treatment or other cleaning treatment are possible on foam glass to potentially restore their photocatalysis power, which is more delicate to realise with the cellulose support.

Therefore, this work shows the real possibility to use industrial waste glass to transform them into photocatalyst support for environmental applications.

Acknowledgements

We thank Ahlstrom research and service (C. Vallet) for supplying photocatalytic non-woven paper media 1049, Cooper Standard Automotive (JM Veillé) Vitré France for glass waste supplying, Arcelor Mittal Dunkerque France (Th. Desmonts) for steel-making ash and smoke, and JF Coulon, ECAM-Rennes for SEM analysis. The undergraduate students F. Boivent, N. Freslon, Th. Reynaldo, M. Toutirais, L. Mougenot, J. Tamakusu are thanked here.

References

[1] G. Scarinci, G. Brusatin, E. Bernardo, Glass foams, in: Schefler, Colombo (Eds.), Cellular Ceramics, WILEY-VCH, 2005, pp. 158–176.

[2] A. Rolland. Thèse de Doctorat n°226, Universtité de Rennes 1(France), (1988).

[3] M. Tasserie, D. Bideau, Y. Laurent, P. Verdier, A new expanded material: optimization of the fabrication process, Journal of High Temperature Chemical Processes 1 (3) (1992) 241–250.

[4] M. Tasserie, D. Bideau, J. Rocherulle, P. Verdier, Y. Laurent, New expanded material based on industrial glass. I. Effect of the quality of powders and their mixing on properties of the material, Verre 6 (1) (1992) 9–15.

[5] Francois Mear, Pascal Yot, Martine Cambon, Renaud Caplain, Michel Ribes, Characterisation of porous glasses prepared from Cathode Ray Tube (CRT), Powder Technology 162 (2006) 59–63.

[6] F. Mear, P. Yot, M. Cambon, M. Ribes, Advances in Applied Ceramics 104 (3) (2005) 123–130.

[7] F. Mear, Thèse de Doctorat n° Université Montpellier 2, France (2004).

[8] E. Bernardo, R. Cedro, M. Florean, S. Hreglich, Reutilization and stabilization of wastes by the production of glass foams, Ceramics International 33 (2007) 963–968.

[9] E. Bernardo, Micro- and macro-cellular sintered glass-ceramics from wastes, Journal of the European Ceramic Society 27 (2007) 2415–2422.

[10] Alejandro Saburit Llaudis, Marıa Jose Orts Tari, Francisco Javier Garcıa Ten, Enrico Bernardo, Paolo Colombo, Foaming of flat glass cullet using Si_3N_4 and MnO_2 powders, Ceramics International 35 (2009) 1953–1959.

[11] E. Bernardo, F. Albertini, Glass foams from dismantled cathode ray tubes, Ceramics International 32 (2006) 603–608.

[12] M. Tasserie, D. Bideau, P. Verdier, Y. Laurent, New expanded material based on industrial glass. II. Role and effect of the amount of an expansive additive on the characteristics of the material, Verre 6 (2) (1992) 103–107.

[13] C. Garnier, J. Razafindrafindrakoto, P. Verdier, Y. Laurent, brevet français, WO 95/35264, Aluminosilicate monolithique expansé à double porosité ouverte, Cernix, France, 1995.

[14] A.I. Shutov, L.I. Yashurkaeva, S.V. Alekseev, T.V. Yashurkaev, Determination of practical properties of heat-insulating foam glass, Glass and Ceramics 65 (2008) 3–5.

[15] Pittsburgh Corning Foamglass Insulation, http://www.foamglasinsulation.com/.

[16] H.R. Fernandes, D.U. Tulyaganov, J.M.F. Ferreira, Preparation and characterization of foams from sheet glass and fly ash using carbonates as foaming agents, Ceramics International 35 (2009) 229–235.

[17] D.U. Tulyaganov, H.R. Fernandes, S. Agathopoulos, J.M.F. Ferreira, Preparation and characterization of high compressive strength foams from sheet glass, Journal of Porous Materials 13 (2006) 133–139.

[18] A.F. Lemos, J.M.F. Ferreira, Materials Science and Engineering: C, C11 (2000) 35–40.

[19] J.P. Wu, A.R. Boccaccini, P.D. Lee, R.D. Rawlings, Thermal and mechanical properties of a foamed glass-ceramic material produced from silicate wastes, European Journal of Glass Science and Technology, Part A Glass Technology 48 (3) (2007) 133–141.

[20] Andrew Mills, Stephen Le Hunte, An overview of semiconductor photocatalysis, Journal of Photochemistry and Photobiology A: Chemistry 108 (1997) 1–35.

[21] J. Calabria A., W.L. Vasconcelos, D.J. Daniel, R. Chater, D. McPhail, Aldo R. Boccaccini, Synthesis of sol–gel titania bactericide coatings on adobe brick, Construction and Building. Materials 24 (3) (2010) 384–389.

[22] Shaobin Wang, H.M. Ang, Moses O. Tade, Volatile organic compounds in indoor environment and photocatalytic oxidation: state of the art, Environment International 33 (2007) 694–705.

[23] A. Strini, S. Cassese, L. Schiavi, Measurement of benzene, toluene, ethylbenzene and o-xylene (BTEX) gas phase photodegradation by titanium dioxide dispersed in cementitious materials using a mixed flow reactor, Applied Catalysis B: Environmental 61 (2005) 90–97.

[24] F. Thevenet, O. Guaïtella, J.M. Herrmann, A. Rousseau, C. Guillard, Photocatalytic degradation of acetylene over various titanium dioxide-based photocatalysts, Applied Catalysis B 61 (2005) 58–68.

[25] A. Aguedach, S. Brosillon, J. Morvan, E.K. Lhadi, Photocatalytic degradation of azo-dyes reactive black 5 and reactive yellow 145 in water over a newly deposited titanium dioxide, Applied Catalysis B 57 (2005) 55–62.

[26] B. Boulinguiez, A. Bouzazaa, S. Merabet, D. Wolbert, Photocatalytic degradation of ammonia and butyric acid in plug-flow reactor: degradation kinetic modeling with contribution of mass transfer, Journal of Photochemistry and Photobiology A: Chemistry 200 (2008) 254–261.

[27] S. Brosillon, L. Lhomme, C. Vallet, A. Bouzaza, D. Wolbert, Gas phase photocatalysis and liquid phase photocatalysis: interdependence and influence of substrate concentration and photon flow on degradation reaction kinetics, Applied Catalysis B: Environmental 78 (2008) 232–241.

[28] S. Lebrette, C. Pagnoux, P. Abélard, Stability of aqueous TiO2 suspensions: influence of ethanol, Journal of Colloid and Interface Science 280 (2) (2004) 400–408.

[29] JCPDS, International Centre for Diffraction data (ICDD), Powder Diffraction File (PDF) #.